Fronto-thalamo-cerebellar circuitry in predicting cognition and behavior of ABCD adolescents

Jiayu Chen[1,2], Sanket Deshpande[2,*], Zening Fu[1,2], Armin Iraji[1,2], Shihao Ji[3], Tricia Z. King[4], Vince D. Calhoun[1,2], Jingyu, Liu[1,2]*

[1]Tri-Institutional Center for Translational Research in Neuroimaging and Data Science (TReNDS), Georgia State University, Georgia Institute of Technology, and Emory University, Atlanta, GA, USA
[2]Department of Computer Science, Georgia State University, Atlanta, GA, USA
[3]School of Computing, University of Connecticut, Storrs, CT, USA
[4]School of Nursing, Emory University, Atlanta, GA, USA
*These authors contributed equally to this work.

ABSTRACT

Attention deficit (AD) is a key symptom dimension in mental health and has been found to present as a continuous trait distributed across the general population and a broad spectrum of mental disorders. However, little is known about how the fronto-thalamo-cerebellar (FTC) circuitry relates to AD, despite having been implicated in AD-related studies. The current work utilized the ABCD data collected at 10 years old to investigate the predictive power of FTC gray and white matter features on various neurocognitive and behavioral measures relevant to AD in the general population. Three different predictive models were trained separately to avoid model-related bias. The results support that gray matter variations in the FTC circuitry more effectively predict working memory performance than the extensively studied FTP circuitry, extending our knowledge on the role of FTC underlying neurocognition and AD.

Index Terms— Working memory, attention, fronto-thalamo-cerebellar, parietal, gray matter, white matter.

1. INTRODUCTION

Attention-deficit (AD), while being recognized as a key symptom of ADHD, has been found to be more likely persist into adulthood than hyperactivity [1, 2]. In addition, evidence supports that rather than being observed exclusively in ADHD, AD presents as a continuous trait distributed across the general population and a broad spectrum of mental disorders including autism spectrum disorder, schizophrenia, and depression[3-5]. These previous findings motivate studying AD from a transdiagnostic perspective with the general population included. An improved understanding of the neuronal basis of AD is expected to inform the underlying biology of a key symptom dimension in mental health, to allow better prediction of AD progression, and to facilitate more precise treatment.

Attention has been widely studied as a key construct of the cognition domain, and is known to involve a constellation of distinct neuronal circuits[6]. Centered on the classic fronto-parietal circuitry, the dorsal and ventral attention networks are considered to play a key role in attention orientation [7]. More recently, there has been growing evidence for the role of the cerebellum in attention. Our previous studies have identified gray matter alterations in cerebellar and frontal regions to be related to inattention and working memory deficits consistently in adolescents and adults with ADHD [2, 8]. We also have found that the white matter tract connecting the right-cerebellum, thalamus and left-frontal regions was linked to auditory attention in survivors of childhood cerebellum tumors[9]. Alterations in the functional connectivity of the frontal and cerebellum regions have also been implicated for associations with attention and working memory deficits in the ADHD and general population [10, 11]. Overall these findings echo the notion that cerebellum is involved in multiple functions, far beyond motor skills [12], and support to examine attention and working memory associations with the frontal-subcortical-cerebellar loops [13, 14], which is made up of the cerebellar connections to the contralateral frontal lobe via the dentate nucleus and thalamus (See Figure 1 in [13]). However, while most investigations of AD to date have focused on fronto-parietal circuities, little is known about how the fronto-thalamo-cerebellar (FTC) circuitry relates to AD, despite the aforementioned evidence. The current work thus aims to investigate how structural alterations in the FTC circuitry are related to AD in comparison with the classic fronto-thalamo-parietal (FTP) circuitry.

As a longitudinal cohort of normally developing adolescents, the Adolescent Brain Cognitive Development (ABCD) [15] study presents an ideal dataset to study the FTC circuitry in relation to AD in the general population. In this work, we focused on the data collected at 10 years old to investigate the predictive power of FTC gray and white matter features on various neurocognitive and behavioral measures relevant to AD, including attention/vigilance, working memory, inattention behavioral, and syndrome scores. Three different predictive models, including Bayesian Ridge Regression (BRR), Neural Network (NN), and Support Vector Regression (SVR) were trained separately to avoid model-

This study is supported by NIH grant: MH130595 to Liu and Ji.
Correspondence: jliu75@gsu.edu.

related bias and allow an objective evaluation of the predictive power of the FTC region, which was further compared with the FTP circuitry and the full fronto-thalamo-parietal-cerebellar (FTPC) circuitry to extend our knowledge on the role of FTC underlying neurocognition and AD.

2. MATERIALS AND METHODS

ABCD cohort and assessment scores. In this study, we utilized the ABCD data release 5.1, where the baseline structural and diffusion-weighted magnetic resonance images (sMRI and dMRI) were trained to predict the selected cognitive and behavioral measures including: (a) The 0-back accuracy (c0b) of the N-back working memory test (i.e., the rate of correct responses to 0 back stimuli) as a measure of attention/vigilance; (b) The 2-back accuracy (c2b) as a measure of working memory performance; (c) The Child Behavior Checklist (CBCL) attention score as a measure of AD behavioral problems; and (d) The top principal component (PC1) extracted from CBCL attention score, Kiddie Schedule for Affective Disorders and Schizophrenia (K-SADS) inattention syndrome, and brief problem monitor-teacher's report attention score, as a measure of the overall AD symptom as in [16]. Table 1 summarizes the sample sizes available for each of the predictions after quality control, along with the N of outer training loop, validation and test.

Table 1: An overview of samples sizes (Cog: c0b, c2b).

	sMRI (N)				dMRI (N)			
	Total	Test	Train	Validation	Total	Test	Train	Validation
Cog	10299	2059	8239	1647	8299	1659	6639	1327
CBCL	10537	2107	8429	1685	8475	1695	6780	1356
PC	6928	1385	5542	1108	5869	1173	4695	939

sMRI preprocessing. T1-weighted sMRI images were preprocessed using the DARTEL tool from the standard statistical parametric mapping 12 (SPM 12) under the MATLAB 2023b environment. Image registration, bias correction, and tissue classification were conducted using the unified model. The DARTEL was used to estimate the gray matter volume (GMV) images, which were then resliced to 1.5 mm resolution, and smoothed by a 3 mm full width at half-maximum Gaussian kernel.

dMRI preprocessing. In brief, preselection of b0 images was conducted by choosing the least-distorted pair, which was subsequently used to estimate the susceptibility-induced off resonance field. The DTI volumes were corrected for eddy current-induced distortions, head movement, and EPI distortions. Additional advanced features in eddy were enabled to further enhance motion correction [17, 18]. Diffusion tensor were calculated using FSL tool *dtifit* with linear regression, resulting in fractional anisotropy (FA) maps which were registered to MNI space using nonlinear registration by ANTs and resliced to 1 mm resolution.

Brain atlas and ROI features. Brain atlases were utilized to identify regions of interests (ROIs) in the FTC and FTP circuitry. Specifically, Schaefer atlas [19] was utilized to map frontal and parietal ROIs. The subcortical atlas proposed by Seitzman et al. [20] was leveraged to map thalamus ROIs. The SUIT hierarchical subcortical atlas [21] was utilized to obtain cerebellum ROIs. We also included a partition of the red nucleus based on the AHEAD database [22], given its role in the proposed frontal-subcortical-cerebellum loop [13, 14]. As a result, for the sMRI GMV images, a total of 335, 304, and 211 ROIs were obtained for the FTPC, FTP, and FTC circuitry, respectively. For the dMRI FA images, the corresponding numbers of ROIs were 341, 310, and 213, respectively. The difference in image resolutions led to different numbers of ROIs. Then for each ROI, we computed the average GMV or FA across all the voxels as the representative ROI feature to be used for prediction.

Predictive Model Training. Nested cross-validation was employed with a structure of 5 outer folds and 5 inner folds to ensure robust model performance across all splits in both test and validation phases, minimizing bias and variance in evaluation. The samples sizes available for training, validation and test can be found in Table 1. The study employed three predictive models to avoid model-related bias in prediction performance: Bayesian Ridge Regression, Support Vector Regression from scikit-learn, and a two-layer Neural Network implemented in PyTorch.

Bayesian Ridge Regression (BRR). This model builds on linear regression by incorporating prior probability distributions over model parameters, enabling it to account for uncertainty in parameter estimates. The model performed effectively with default settings. The feature importance scores were calculated based on the coefficients for each feature learned through the training.

Support Vector Regression (SVR). A Bayesian search was conducted to optimize the regularization parameter by maximizing validation r^2 values (variance explained). Among the linear, Radius basis function (RBF), and polynomial kernels, RBF yielded the best performance and was hence reported here. The feature importance scores were calculated using the permutation method, which quantifies the feature importance by measuring the decrease in model performance when that feature's values are randomly shuffled.

Neural Network (NN). This model consisted of two hidden layers with 128 and 64 units, respectively, and included dropout of 0.2. The learning rate for each target variable was selected through the nested cross-validation grid search, with values ranging from 1E-06 to 5E-05, with a learning rate decay by 0.5 if no improvement observed in validation R^2 after 10 epochs. The feature importances were assessed by calculating the gradient of the model's output with respect to each input feature after training.

Meta-analysis on brain circuitry differences. The performance of prediction was evaluated by the correlation between the predicted and original scores in each test fold. We conducted meta-analysis to compare FTC's prediction performance with those of FTP and FTPC across all the predictive models and test/validation folds (i.e., N = 180 observations in each analysis). The inverse variance algorithm implemented in PythonMeta tool was used for the analysis with mean difference as the effect measure.

3. RESULTS

Tables 2 and 3 summarize the prediction performance of GMV and FA features for c0b (vigilance), c2b (working memory), CBCL behavior score, and PC1 attention symptom scores, respectively. In each table, the prediction r^2 and correlation values are reported for the performance of three circuitries using three different predictive models. The predictive models (BRR, SVR, NN) presented similar results and none could outperform others in all the tests.

Table 2: Prediction performance of GMV features.

c0b	**Prediction**	**FTPC**	**FTP**	**FTC**
BRR	r^2	0.049 ± 0.009	0.045 ± 0.009	0.046 ± 0.009
	Corr	0.222 ± 0.019	0.214 ± 0.020	0.217 ± 0.019
SVR	r^2	0.054 ± 0.007	0.049 ± 0.006	0.052 ± 0.007
	Corr	0.249 ± 0.024	0.238 ± 0.020	0.244 ± 0.023
NN	r^2	0.048 ± 0.008	0.046 ± 0.009	0.046 ± 0.009
	Corr	0.221 ± 0.017	0.217 ± 0.020	0.216 ± 0.020
c2b	**Prediction**	**FTPC**	**FTP**	**FTC**
BRR	r^2	0.054 ± 0.005	0.050 ± 0.005	0.052 ± 0.006
	Corr	0.234 ± 0.009	0.225 ± 0.011	0.230 ± 0.013
SVR	r^2	0.062 ± 0.008	0.058 ± 0.006	0.061 ± 0.007
	Corr	0.262 ± 0.018	0.254 ± 0.017	0.259 ± 0.018
NN	r^2	0.056 ± 0.005	0.050 ± 0.006	0.055 ± 0.008
	Corr	0.237 ± 0.011	0.226 ± 0.014	0.236 ± 0.017
CBCL	**Prediction**	**FTPC**	**FTP**	**FTC**
BRR	r^2	0.009 ± 0.002	0.008 ± 0.003	0.009 ± 0.003
	Corr	0.099 ± 0.015	0.094 ± 0.018	0.098 ± 0.019
SVR	r^2	-0.091 ± 0.000	-0.092 ± 0.000	-0.116 ± 0.002
	Corr	0.081 ± 0.027	0.083 ± 0.030	0.083 ± 0.006
NN	r^2	0.005 ± 0.004	0.007 ± 0.005	0.004 ± 0.004
	Corr	0.084 ± 0.023	0.084 ± 0.033	0.071 ± 0.031
PC1	**Prediction**	**FTPC**	**FTP**	**FTC**
BRR	r^2	0.013 ± 0.008	0.012 ± 0.007	0.012 ± 0.006
	Corr	0.123 ± 0.031	0.119 ± 0.029	0.117 ± 0.022
SVR	r^2	-0.115 ± 0.003	-0.116 ± 0.000	-0.122 ± 0.003
	Corr	0.094 ± 0.005	0.092 ± 0.002	0.077 ± 0.016
NN	r^2	0.016 ± 0.006	0.010 ± 0.008	0.009 ± 0.006
	Corr	0.128 ± 0.027	0.102 ± 0.037	0.099 ± 0.028

Table 3: Prediction performance of FA features.

c0b	**Prediction**	**FTPC**	**FTP**	**FTC**
BRR	r^2	0.038 ± 0.006	0.037 ± 0.005	0.033 ± 0.006
	Corr	0.198 ± 0.012	0.197 ± 0.009	0.185 ± 0.013
SVR	r^2	0.034 ± 0.007	0.034 ± 0.007	0.027 ± 0.007
	Corr	0.191 ± 0.023	0.191 ± 0.025	0.175 ± 0.021
NN	r^2	0.035 ± 0.009	0.034 ± 0.004	0.030 ± 0.009
	Corr	0.192 ± 0.022	0.186 ± 0.008	0.180 ± 0.020
c2b	**Prediction**	**FTPC**	**FTP**	**FTC**
BRR	r^2	0.044 ± 0.006	0.043 ± 0.006	0.037 ± 0.008
	Corr	0.214 ± 0.011	0.212 ± 0.010	0.198 ± 0.014
SVR	r^2	0.042 ± 0.005	0.042 ± 0.005	0.032 ± 0.003
	Corr	0.219 ± 0.015	0.219 ± 0.015	0.195 ± 0.010
NN	r^2	0.039 ± 0.006	0.036 ± 0.009	0.037 ± 0.009
	Corr	0.205 ± 0.010	0.187 ± 0.021	0.196 ± 0.012
CBCL	**Prediction**	**FTPC**	**FTP**	**FTC**
BRR	r^2	0.007 ± 0.004	0.005 ± 0.004	0.004 ± 0.003
	Corr	0.091 ± 0.025	0.083 ± 0.027	0.072 ± 0.021
SVR	r^2	-0.126 ± 0.006	-0.126 ± 0.007	-0.129 ± 0.005
	Corr	0.058 ± 0.021	0.055 ± 0.023	0.043 ± 0.028
NN	r^2	0.005 ± 0.006	0.002 ± 0.008	-0.001 ± 0.010
	Corr	0.074 ± 0.037	0.059 ± 0.041	0.048 ± 0.031
PC1	**Prediction**	**FTPC**	**FTP**	**FTC**
BRR	r^2	0.013 ± 0.008	0.011 ± 0.007	0.007 ± 0.008
	Corr	0.119 ± 0.031	0.113 ± 0.031	0.095 ± 0.035
SVR	r^2	-0.114 ± 0.002	-0.127 ± 0.007	-0.114 ± 0.003
	Corr	0.094 ± 0.008	0.055 ± 0.023	0.096 ± 0.010
NN	r^2	0.013 ± 0.002	0.009 ± 0.004	0.003 ± 0.001
	Corr	0.115 ± 0.030	0.099 ± 0.042	0.058 ± 0.021

Table 4 summarizes the meta-analyses of differences in prediction performance between the three brain circuitries. We focused our analysis on the prediction of c0b and c2b as the brain features can more reliably predict these two cognitive measures as demonstrated in Tables 2 and 3.

Table 4: Meta-analysis on differences between brain circuitries.

Target	**Comparison**	GMV		FA	
		Z score	**P value**	**Z score**	**P value**
c0b	FTPC vs FTP	4.5	<0.001	1.23	0.219
	FTPC vs FTC	3.89	<0.001	10.78	<0.001
	FTC vs FTP	0.74	0.459	-12.12	<0.001
c2b	FTPC vs FTP	11	<0.001	1.97	0.048
	FTPC vs FTC	6.45	<0.001	11.86	<0.001
	FTC vs FTP	2.24	0.029	-12.14	<0.001

Based on the kneeling point of feature importance, we examined the top 20 important ROIs for each model. Given that our research focus was the role of the cerebellum in the context of the frontal and parietal regions, and that GMV features more reliably and robustly predicted cognitive measures (Table 2), we focused our interpretation on the top ROIs identified from the full FTPC circuitry when using GMV to predict c0b and c2b. Figure 1 shows the top ROIs identified in BRR, SVR, and NN models for c0b and c2b respectively. The top ROIs were distributed across the frontal, parietal, and cerebellum regions. ROIs identified in all three models included: red nucleus, right insula, left inferior frontal, and right anterior cingulate regions for both c0b and c2b; left middle frontal regions for c0b; as well as right superior frontal, right angular gyrus, right thalamus, and right cerebellum VI and VIII regions for c2b. Besides, the second most identified cerebellum ROIs, right crus II and right crus I were labeled as top important in three out of six trained models.

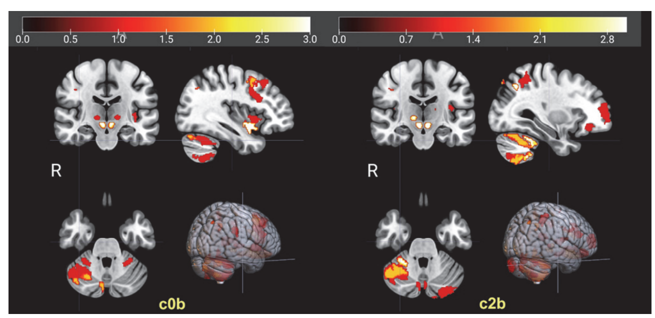

Figure 1: The top ROIs of FTPC model for c0b (left) and c2b (right). The color code (1, 2, and 3) indicates how many times the ROI was identified across BRR, SVR and NN models.

4. DISCUSSION AND CONCLUSION

This work represents an initial effort to understand the role of the FTC circuitry in attention problems and related cognitive processes in youth using the initial ABCD dataset. Overall, regardless of predictive models, both GMV and FA features were more capable of predicting cognitive performance (c0b and c2b) than behavioral measures (CBCL and PC1). For most of the cases, the full FTPC circuitry outperformed FTP and FTC in predicting either cognitive or behavioral measures, with only one exception (GMV features predicting CBCL using SVR). The meta-analysis confirmed superior performance of FTPC compared to FTP or FTC, where the

FTPC circuitry significantly outperformed the FTP and FTC circuitry in predicting both c0b and c2b. These results indicate that all four brain regions (frontal, thalamus, parietal, and cerebellar) are involved in cognitive performance or behavioral scores, yet with different contributions.

Our meta-analysis also shows the support that GMV variations in the FTC circuitry more effectively predict working memory performance than the extensively studied FTP circuitry, as FTC presented a significantly higher prediction accuracy for c2b compared to FTP, while there is no difference in prediction of c0b. The consistently identified top ROIs echo the performance. Particularly, the top consistent cerebellum ROI (anatomical cerebellum VI and VIII) have been labeled as functionally related to spatial simulation in the SUIT hierarchical atlas [21]. It is also worth noting the second most identified cerebellum ROIs, right crus I and crus II are considered functionally related to spatial and verbal working memory in the SUIT atlas [21], which resonates with their contribution in predicting attention and working memory.

In contrast, while comparing FA features in the performance of FTC, FTP, and FTPC circuitries, FTP is significantly better than FTC, and FTPC performs comparable to FTP in the prediction of C0b, but better in C2b, suggesting a certain level of cerebellar contribution to working memory, but less than parietal regions. The suboptimal performance from FA features, compared to GMV, in predicting cognitive and behavioral scores warrants further studies. One speculation is that the FA features extracted with cortical brain atlas might not well capture the full body of white matter variations, in particular white matter tract-based features.

In conclusion, our work lends support for an important role of the cerebellum in neurocognition, motivating further delineation of the FTC circuitry for their impact on AD.

5. REFERENCES

[1] T. J. Spencer, J. Biederman, and E. Mick, "Attention-deficit/hyperactivity disorder: diagnosis, lifespan, comorbidities, and neurobiology," (in eng), *J. Pediatr. Psychol.,* Review vol. 32, no. 6, pp. 631-42, Jul 2007.

[2] J. Liu *et al.*, "Gray matter networks associated with cognitive deficit in ADHD across adolescence and adulthood," *Transl Psychiatry,* vol. in press, 2021.

[3] C. Lord *et al.*, "Autism spectrum disorder," *Nat Rev Dis Primers,* vol. 6, no. 1, p. 5, Jan 16 2020.

[4] R. S. Keefe and P. D. Harvey, "Cognitive impairment in schizophrenia," (in eng), *Handb. Exp. Pharmacol.,* no. 213, pp. 11-37, 2012.

[5] X. Wang, H. Zhou, and X. Zhu, "Attention deficits in adults with Major depressive disorder: A systematic review and meta-analysis," *Asian J Psychiatr,* vol. 53, p. 102359, Oct 2020.

[6] A. Raz, "Anatomy of attentional networks," *Anat. Rec. B. New Anat.,* vol. 281, no. 1, pp. 21-36, Nov 2004.

[7] J. T. Bowling, K. J. Friston, and J. B. Hopfinger, "Top-down versus bottom-up attention differentially modulate frontal-parietal connectivity," *Hum Brain Mapp,* vol. 41, no. 4, pp. 928-942, Mar 2020.

[8] K. Duan *et al.*, "Neural correlates of cognitive function and symptoms in attention-deficit/hyperactivity disorder in adults," (in eng), *Neuroimage Clin,* vol. 19, pp. 374-383, 2018.

[9] A. S. Ailion *et al.*, "Double Dissociation of Auditory Attention Span and Visual Attention in Long-Term Survivors of Childhood Cerebellar Tumor: A Deterministic Tractography Study of the Cerebellar-Frontal and the Superior Longitudinal Fasciculus Pathways," *J. Int. Neuropsychol. Soc.,* vol. 26, no. 10, pp. 939-953, Nov 2020.

[10] Sarah Johnson *et al.*, "Effects of Functional Connectivity on ADHD Relevant Traits during the Normal Developmental Phase," presented at the OHBM, Virtual, 2020. [Online]. Available.

[11] S. Wang, Y. Yang, W. Xing, J. Chen, C. Liu, and X. Luo, "Altered neural circuits related to sustained attention and executive control in children with ADHD: an event-related fMRI study," *Clin. Neurophysiol.,* vol. 124, no. 11, pp. 2181-90, Nov 2013.

[12] G. Castellazzi *et al.*, "Prominent Changes in Cerebro-Cerebellar Functional Connectivity During Continuous Cognitive Processing," *Front Cell Neurosci,* vol. 12, p. 331, 2018.

[13] S. V. Clark, E. S. Semmel, H. A. Aleksonis, S. N. Steinberg, and T. Z. King, "Cerebellar-Subcortical-Cortical Systems as Modulators of Cognitive Functions," *Neuropsychol. Rev.,* Jan 29 2021.

[14] S. N. Steinberg, J. P. Greenfield, and K. Perrine, "Neuroanatomic Correlates for the Neuropsychological Manifestations of Chiari Malformation Type I," *World Neurosurg,* vol. 136, pp. 462-469, Apr 2020.

[15] N. D. Volkow *et al.*, "The conception of the ABCD study: From substance use to a broad NIH collaboration," *Dev Cogn Neurosci,* vol. 32, pp. 4-7, Aug 2018.

[16] M. M. Cordova *et al.*, "Attention-Deficit/Hyperactivity Disorder: Restricted Phenotypes Prevalence, Comorbidity, and Polygenic Risk Sensitivity in the ABCD Baseline Cohort," *J Am Acad Child Adolesc Psychiatry,* vol. 61, no. 10, pp. 1273-1284, Oct 2022.

[17] J. L. Andersson, M. S. Graham, E. Zsoldos, and S. N. Sotiropoulos, "Incorporating outlier detection and replacement into a non-parametric framework for movement and distortion correction of diffusion MR images," *Neuroimage,* vol. 141, pp. 556-572, 2016.

[18] J. L. Andersson, M. S. Graham, I. Drobnjak, H. Zhang, N. Filippini, and M. Bastiani, "Towards a comprehensive framework for movement and distortion correction of diffusion MR images: Within volume movement," *Neuroimage,* vol. 152, pp. 450-466, 2017.

[19] A. Schaefer *et al.*, "Local-Global Parcellation of the Human Cerebral Cortex from Intrinsic Functional Connectivity MRI," *Cereb Cortex,* vol. 28, no. 9, pp. 3095-3114, Sep 1 2018.

[20] B. A. Seitzman *et al.*, "A set of functionally-defined brain regions with improved representation of the subcortex and cerebellum," *Neuroimage,* vol. 206, p. 116290, Feb 1 2020.

[21] C. Nettekoven *et al.*, "A hierarchical atlas of the human cerebellum for functional precision mapping," *Nat Commun,* vol. 15, no. 1, p. 8376, Sep 27 2024.

[22] A. Alkemade *et al.*, "The Amsterdam Ultra-high field adult lifespan database (AHEAD): A freely available multimodal 7 Tesla submillimeter magnetic resonance imaging database," *Neuroimage,* vol. 221, p. 117200, Nov 1 2020.